POLITECNICO MILANO 1863

SCUOLA DI INGEGNERIA INDUSTRIALE E DELL'INFORMAZIONE

EXECUTIVE SUMMARY OF THE THESIS

MULTI-CONDUCTOR WINDINGS FOR HIGH-FREQUENCY ELECTRIC MOTORS

TESI MAGISTRALE IN ELECTRICAL ENGINEERING – INGEGNERIA ELETTRICA

AUTHOR: JURI TESSARO

ADVISOR: MATTEO FELICE IACCHETTI

ACADEMIC YEAR: 2022-2023

1. Introduction

This thesis focuses on the reduction of AC losses in windings for high-frequency (500 Hz – 2.0 kHz) electric motors. Such "motor-wise" high-frequency levels are required in order to increase the rated speed and the number of poles, thereby reducing the overall motor mass. This aspect is particularly relevant to the automotive and aerospace sectors, where compactness and high-power density are key factors [4].

The research concentrates on the design of windings suitable for high frequencies, capable of meeting the required power specifications and limiting additional losses. Various types of windings are analysed, with special attention given to both Hairpin and concentrated-coil windings with a few turns per slot as required in high-speed low-voltage applications. The idea of subdividing the coil conductors is introduced to determine the optimal arrangement for limiting current circulation between parallel conductors and reducing high-frequency losses. For high frequencies (above 1 kHz), the possibility of using flat conductors made entirely of Litz wire is examined.

2. Winding and Losses

4.3 Windings:

For electric motors, there are different types of windings used, each with specific characteristics that influence the motor's performance. The choice of the winding type depends on the specific application requirements and the desired motor characteristics. Winding design takes into account factors such as current distribution, space-harmonics, and cooling. Therefore, understanding the different windings is essential for controlling and optimizing motor performance, enabling efficient electromechanical energy conversion.

Among the various types of windings used in automotive, the most common and widespread ones are random wire windings Figure 2.1 (a), and Hairpin windings Figure 2.1 (b). In a random wire winding each turn is formed by one or more thin wires in parallel, randomly arranged within the slot. Hairpin windings features solid bar conductors with hairpin-like shape, which create single turns and are inserted directly into the motor slots, welded together to form a single winding that spans over the entire stator belt.

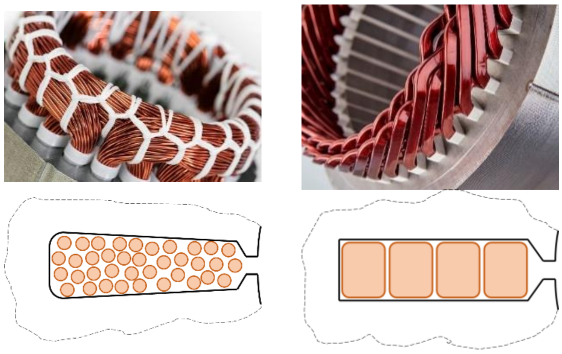

Figure 2.1: Random winding (a) and Hairpin winding (b)

The winding fill factor relative to the slot size is defined, as the ratio of the surface area occupied by the conductor to that of the slot:

$$K_{fill} = \frac{S_{Cu}}{S_{cava}} \tag{2.1}$$

Hairpin windings use solid rectangular conductors and are typically placed in rectangular slots to improve the fill factor. They can achieve a higher fill factor compared to random windings, making them particularly attractive for applications at high current density. This can be appreciated in Figure 2.1. A high fill-factor also improves the heat rejection though the potting, which again helps enabling higher current density.
An important characteristic of Hairpin elements is related with by the geometry they assume on the coil ends. A partial natural transposition of the conductor assembly can be achieved due to the orientation reversing at the 180° bend, Figure 2.2.

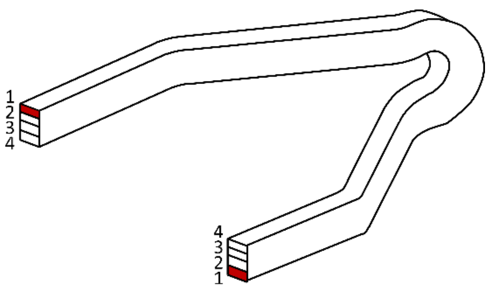

Figure 2.2: Hairpin end-winding

One of the goals of this study, was to assess if this transposition can be effective and evenly distribute the current among the individual sub-conductors.

4.4 Losses:

Losses in the windings of an electric machine refer to the power dissipated as heat, due to Joule effect caused by the current during operation.
The conduction field in electric machine windings is complex, and under variable conditions, it exhibits numerous effects that make the current distribution non-uniform. A fundamental distinction is made between direct current (DC) losses and alternating current (AC) losses.
DC losses can be expressed by the definition of DC resistance, which depends only on the geometry and the material of the conductors:

$$\mathrm{R_{DC}} = \frac{l}{\sigma\, S} \tag{2.2}$$

The loss associated with this resistance is given by:

$$P_{DC} = R_{DC} I^2 \tag{2.3}$$

On the other hand, alternating current generates varying magnetic fields that link with the conductor, inducing voltages within it, resulting in so-called eddy currents. These eddy currents increase the dissipated power ($P_{AC} > P_{DC}$) due to Joule heating. To account for the increased losses compared to DC regimen, a coefficient k_R is introduced according to the equation:

$$P_{AC} = P_{DC} + \Delta P = k_R \cdot P_{DC} \quad , \quad k_R > 1 \tag{2.4}$$

The main causes of increased losses in AC windings are essentially attributed to two main effects: skin effect and proximity effect.
The skin effect is a phenomenon that caused by the interaction between the alternating current and the magnetic field it generates within itself.
The proximity effect is a phenomenon that occurs when an alternating magnetic field, created outside the conductor, passes through it and induces parasitic currents inside.
Both effects can cause a non-uniform redistribution of current, with a concentration of current in certain regions and a consequent increase in losses. Only simple conductor geometries ad arrangement such as a cylindrical conductor in air allow relatively simple analytical description and separation of these two effects, Figure 2.3.

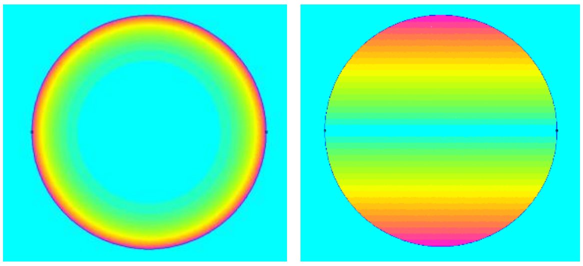

(a) (b)

Figure 2.3: examples of Skin (a) and proximity (b) effect in a cylindrical conductor in air

However, actual winding conductor constitute a far more complex system making a purely analytic approach impractical, then calling for numeric simulations.

3. Methodology

To study the electrical-magnetic system in frequency, the FEMM program was used, which is a free open-source software used to analyse the behaviour of 2D magnetic systems using the Finite Element Method (FEM). In particular, the time-harmonic analysis approach was adopted. This approach allows computing the currents distribution inside the conductors and calculating the associated losses.

It is important to consider some limitations of FEMM package, and the related countermeasures which were put in place to overcome these:

• in order to improve the accuracy of core loss computation, FEMM automatically scales the B-H curve when switching from a direct current (DC) to an alternating current (AC) time-harmonic simulation. However, this comes at the expense of accuracy in the leakage field in slots, and this feature cannot be "turned off" in the software. Therefore, an algorithm to modify the input B-H curve was proposed in order to compensate for FEMM pre-scaling and improve the accuracy of leakage field computation in AC.

• The time harmonic approach does not allow an easy incorporation of rotating Permanent Magnet (PM) fields. However, there is a general consensus that the impact of PM fields on winding eddy-losses can be ignored if the core saturation levels are not too high and this approximation was invoked in the study.

• FEMM cannot represent combinations of parallel and series circuits. Therefore, a hybrid FEA-Analytical/Circuital approach was developed and coded in a MATLAB automatic routine. The flowchart is presented in Figure 3.1:

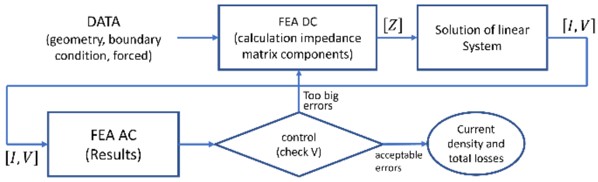

Figure 3.1: block diagram of the proposed hybrid FEM-circuit routine

First, the geometry is imported into FEMM and calculations are carried out to derive the resistances and inductances of the conductors in DC. Next, the circuit linear system formulated by imposing the necessary conditions for parallel connections and subsequently solved. The resulting circuit currents, are then fed back into FEMM to conduct an AC analysis, compute losses and cross check that resulting circuit voltage are within tolerance with those from the circuit solution.

• Simulations of windings consisting of numerous strands/filaments would require significant computational time. To circumvent this problem winding homogenization techniques were invoked [2] [3], as illustrated in Figure 3.2, where the actual multi-strand coil-side is replaced by a homogenised region with appropriate equivalent complex conductivity and permeability.

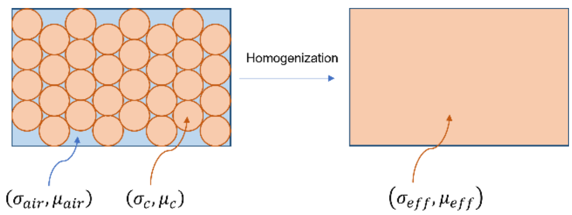

Figure 3.2: Homogenization

4. Case Study Application

4.1 Original Winding and Hairpin Winding

In this study, we explore the application case of the design on the electric motor of the Nissan Leaf (2012 version), a well-established electric vehicle model in the market, Figure 4.1, often used as a benchmark in many studies.

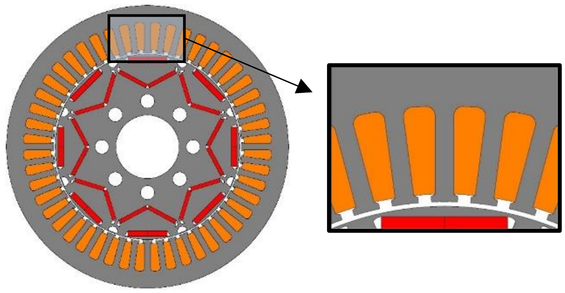

Figure 4.1: Original Nissan Leaf 2012 motor

This motor is designed with a fully-pitched winding composed of random wire. Specifically, each slot consists of six turns, and each turn consists of twenty strands with a diameter of 0.8 mm intertwined together.

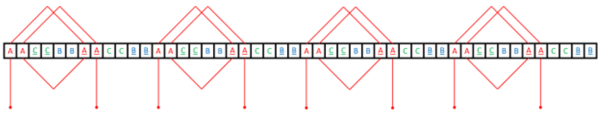

Figure 4.2: Nissan Leaf winding

As a first case-study, the original winding was replaced with a hairpin winding. In order to accommodate this, modifications were made to the stator slots to make them rectangular. Specifically, the width of the slot was kept constant along its entire length, corresponding to the narrower part of the original slot. With this modification, the area of the slot decreases as observed in Figure 4.3. However, with this type of winding, it can be utilized more effectively.

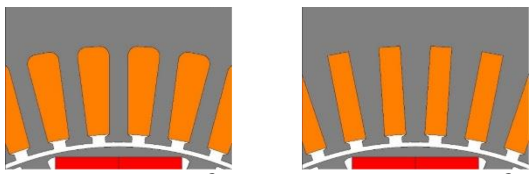

$S_{cu} = 60.32\ mm^2$ $K_{fill} = 52.82\%$

$S_{cu} = 75{,}15\ mm^2$ $K_{fill} = 82.11\%$

Figure 4.3: difference in the slot geometry

In order to compare the different types of windings, an attempt was made to maintain the same configuration of 6 turns per slot, which corresponds to 6 conductors in the slot for the Hairpin winding, and only change the conductor type. The winding was designed as described above and is illustrated in [5].

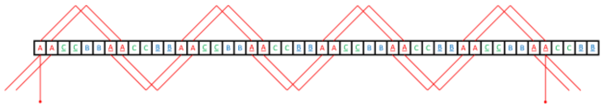

Figure 4.4: Hairpin Winding

One pole of the resulting stator is, formed by the six conductors in the slot, and is shown in Figure 4.5 (a). The 6 conductors have been further divided into n sub-conductors in parallel. An example with three sub-conductors ($n = 3$) and six macro-conductors is shown in Figure 4.5 (b), where different macro-conductors are highlighted with light/dark colours for better distinction.

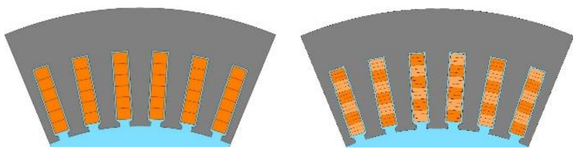

(a) (b)

Figure 4.5: sub-conductor examples

Considering that the flux mostly crosses the slot in the transverse direction, in order to reduce losses, it is necessary to divide the conductors and orient them with the smaller side along the slot height direction.
For the purpose of the analyses, the macro-conductors were subdivided, and their dimensions were calculated as listed in Table 1.

Table 1: sub-conductors dimensions

n	$h_{c,sub}$ [mm]	$b_{c,sub}$ $[mm]$
2	1.56	4.01
3	1.04	4.01
4	0.78	4.01

Here are the results of various simulations at a frequency of 1 kHz with an increasing number of conductor divisions in the slot, highlighting the importance of natural conductor transposition.
In the results shown in Table 2, which display the values of power dissipated by the active sides of the Hairpin and Composite Hairpin windings for each analysis.

Table 2: results power losses at 1 kHz

n	$P_J\ [kW]$ Without transposition	$P_J\ [kW]$ With transposition
1	8.2	8.2
2	7.1	2.8
3	6.7	1.6
4	6.5	1.2

As the number of sub-conductors increases and natural transpositions at the ends are applied to balance the currents in the sub-conductors, the current density becomes increasingly uniform, as can be observed from FIGURE 4.6 and Figure 4.7, which depict the current density along the slot height for $n = 1$ and $n = 4$ with transposition.

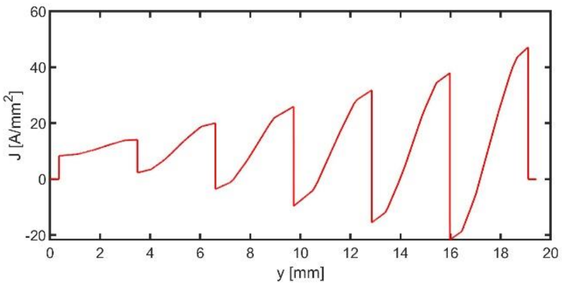

Figure 4.6: current density along the slot height for $n = 1$

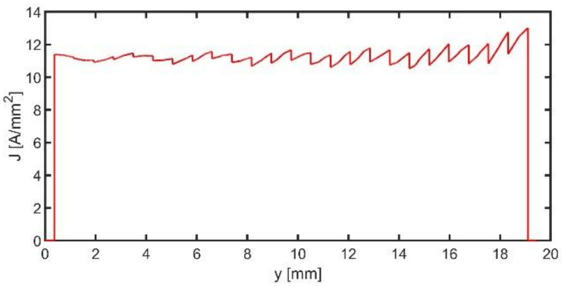

Figure 4.7: current density along the slot height for $n = 4$ and transposition

One significant aspect that emerges from this observation is the positive effect resulting from a uniform distribution of currents. In fact, this uniformity leads to a reduction in losses compared to the basic Hairpin winding.
If the required dimensions of the sub-conductors become too small compared to the available ones, or if further loss reduction is desired in high-frequency windings, the use of Litz conductors must be considered.
Figure 4.8 shows the losses of different windings and conductor sub-division at different frequencies. In the graph of Figure 4.8, a comparison has been included with Litz wire with a strand diameter of 0.2 mm.

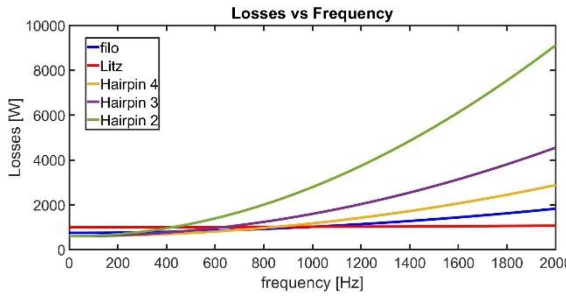

Figure 4.8: losses at different frequencies

The graph in Figure 4.8 shows how the choice of winding depends on the operating frequency. The Hairpin winding can be a good solution at low frequencies, the use of Litz conductors proves advantageous at high frequencies, while the original wire conductor represents an intermediate solution. With proper optimization of the Composite Hairpin winding, further improvements in high-frequency performance can be achieved. In particular, it can be observed that the Composite Hairpin winding is more favourable almost up to frequencies of one kilohertz.

4.2 Concentrated coil Winding

The original Nissan Leaf motor stator was adapted and modified to host a non-overlapped concentrated coil winding, based on fractional slot winding (FSW) layout, Figure 4.9 and Figure 4.10. It is important to emphasize that this modification was not made to compare the performance between the two types of machines but rather to have a reference model with concentrated coil winding for conducting analyses among the different possible connections of the sub-conductors in parallel. Concentrated coil windings offer greater simplicity in construction compared to distributed windings. Another advantage is the reduction in conductor length on the coil ends, resulting in savings of conductor material and hence lower loss reductions. The challenge here is how to realise conductor subdivision and transposition for loss reductio in coils with a very low number of turns (e.g. six turns) required for low-voltage, high-speed applications.

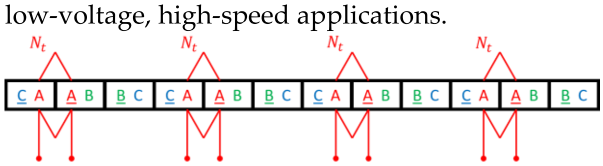

Figure 4.9: Fractional slot winding

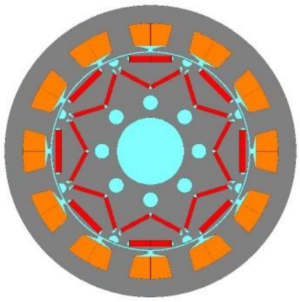

Figure 4.10: Nissan Leaf motor modification with concentrated coils

Concentrated coils are assumed to be made of conductors composed of Litz wire, with a filling factor of approximately 60% for each conductor and a diameter of the individual filament of 0.4 mm. Here, the coil ends of a coil resemble those in a Hairpin, as shown in Figure 2.2, in order to chieve a partial transposition.

The idea is to divide the Litz-Hairpin into different sub-conductors in order to obtain a more flexible conductor, thereby facilitating its insertion and winding inside the stator slots. The conducted analyses focus on finding the best arrangement of the conductors and the most suitable transposition. Figure 4.11 demonstrates how, by rotating the macro-conductors, the sub-conductors are reversed. In Figure 4.11, and in the following figures, the ordered winding turns will be represented in green in one order, while in red in the opposite order.

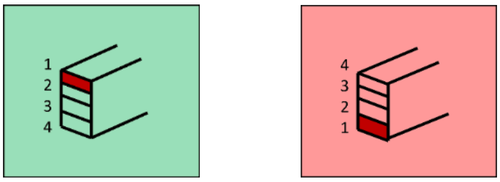

Figure 4.11: example of transposition

In the design of these transpositions, of concentrated coils, three possible configurations can be identified as shown in Figure 4.12. They follow form appropriate rotation of the macro-conductors of the different turns at their ends.

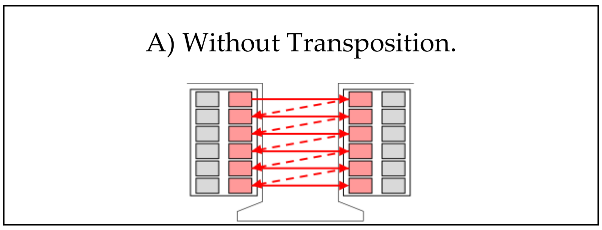

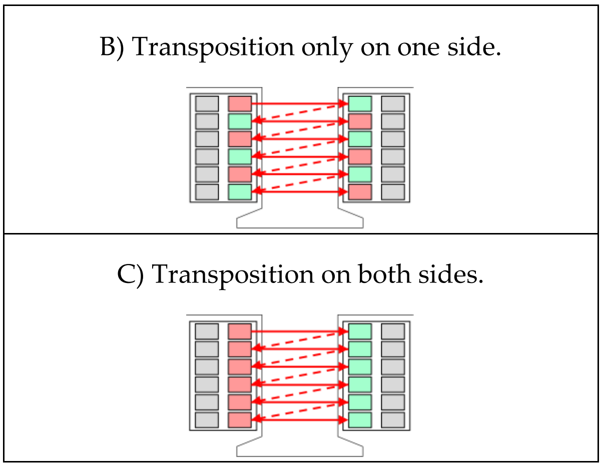

Figure 4.12: possible configurations

Three possible ways of winding the tooth to create the coil have been identified. These methods are qualitatively represented in Figure 4.13. In each case, 3 turns (3 macro-conductors) were considered, each consisting of 4 sub-conductors.

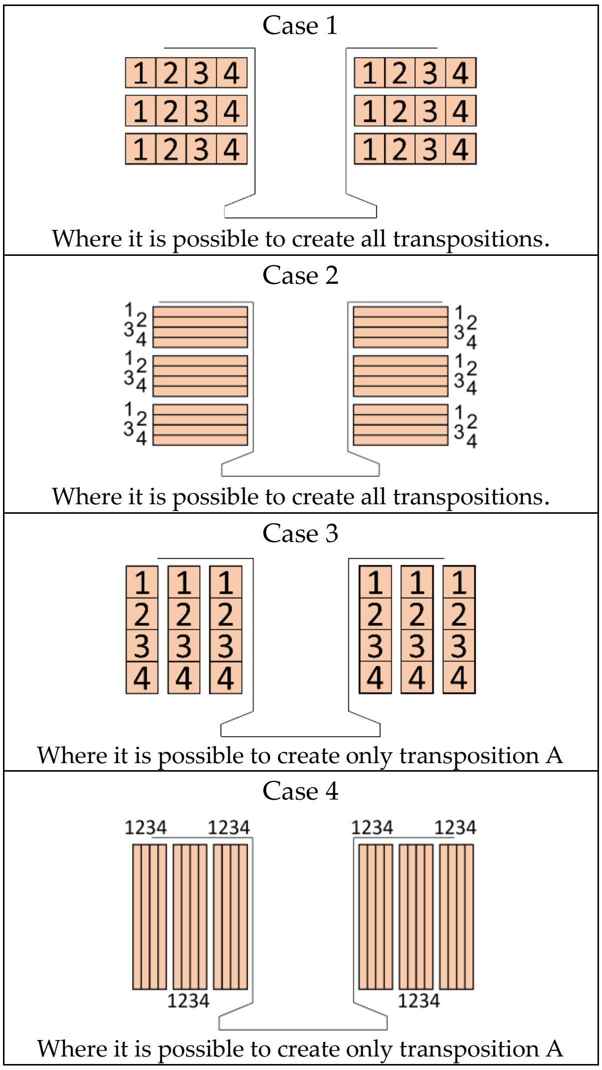

Figure 4.13: Possible ways of winding

Clearly, the above configurations require suitable coil leads to get access to the inner coil starts & ends which are to be properly designed and arranged.
These configurations were analysed with the hybrid FEA-circuital approach developed and discussed in previous Section 3. Figure 4.14 shows the current density maps of configuration 1-B, with the transposition done on only one side of the coil head.

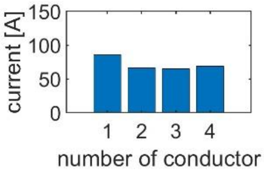

Figure 4.14: current density configuration 1-B

Table 3 collects the values of power dissipated by the winding for each layout. The last row in the table reports the loss value in the case where the same transport current is forced through the sub-conductors. This ideal case leads to the minimum achievable loss value and is used as a reference.

Table 3: Power losses

	Case 1	Case 2	Case 3	Case 4
	***P* [W]**	***P* [W]**	***P* [W]**	***P* [W]**
Without Transposition	469	737	900	398
Transposition only on one side	320	364	/	/
Transposition on both sides	342	373	/	/
Ideal Case	308			

From Table 8, it can be observed that the best "practical" transposition appears to be the one in case 1, with the transposition done on only one side of the coil head (B), while no transposition can lead to very high additional losses.

5 Characterization of losses

The final part of the project was devoted to identify possible test procedures to separate AC losses and validate the proposed winding loss calculation tool. The motor losses can be divided into four main components:
- Joule losses in the windings (P_J)
- Losses in ferromagnetic materials (P_{Fe})
- Mechanical losses (P_m)
- Ventilation losses (P_v)

$$P_{tot} = P_{Joule} + P_{Fe} + P_m + P_v \quad (5.1)$$

An idea to separate AC winding losses is to construct two identical machines, except for the realization of the windings, which have identical configuration and fata but different types of conductors. The first stator (Actual Machine) hosts the actual winding with the selected conductors, while the second stator (Ancillary Machine) adopts a winding can be made of Litz conductors with a sufficiently small strand diameter to have negligible AC losses.
Both stators can be tested by measuring the total terminal power, primarily consisting of two contributions: windings P_J and core P_{Fe} losses.

$$P_{tot} = P_J + P_{Fe} \quad (5.2)$$

In the ancillary stator, P_J is replaced by P_{Litz} which can be estimated as:

$$P_{Litz} = 3R_{Litz} \cdot I^2 \quad (5.3)$$

Where R_{Litz} can be measured through a DC test. Consequently, the core losses are obtained from:

$$P_{Fe} = P_{tot} - P_{Litz} \quad (5.4)$$

Once core losses are estimated form (4.5), it is then possible to power the machine with the actual winding under test and separate winding AC losses as follows:

$$P_{J,AC} = P_{tot} - P_{Fe} - 3R_{DC}I^2 \quad (5.5)$$

Where R_{DC} is the actual winding DC resistance from a DC test.
A similar principle can be applied to a reduced-scale test-bench with the purpose to validate the proposed calculation tool for hairpin elements made of subdivided conductors. It was then decided to design a reduced test bench to prove that the proposed simplified modelling techniques are adequate and can be used on the actual motor as well. Therefore, a “linear” apparatus was designed, consisting of a single coil with a geometry that reproduces slot conditions similar to those in the Nissan Leaf motor, as shown in Figure 4.15, and capable of implementing some transpositions on the coil ends, as shown in Figure 4.16. Table 4 collects the test rig simulated

performance data and loss components, revealing a decent AC winding to total rig loss ratio.
Unfortunately, due to lead times and delays in the supply of custom-designed steel laminations required for the test bench, it was not possible to build the rig on time and carry out the experimental measurements. This activity should undoubtedly be the first one to conduct before future developments on the subject.

Table 4: loss components

	Without Transposition	With Transposition
P_{DC} 2D $[W]$	23	23
P_{DC} 3D $[W]$	37	37
P_{Fe} $[W]$	14	15
P_{AC} 2D $[W]$	328	74
P_{DC} $end - winding$ $[W]$	14	14
P_{tot} $[W]$	356	103

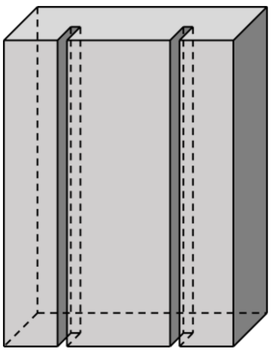

Figure 5.1: Reduced Test-rig laminated stack

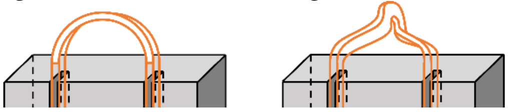

Figure 5.2: Test-rig end-winding

6 Conclusions:

In this thesis a calculation tool for winding AC losses has been proposed and some methods to reduces AC losses in high-frequency (500 Hz – 2.0 kHz) electric motor windings have been explored. Typically, standard random wire windings can limit AC losses, but they achieve poor fill factor. On the other hand, Hairpin windings make more efficient use of the available space in the slot but suffer from high AC losses if the frequency exceed a few hundred hertz.
The research focused on subdividing the Hairpin conductors to achieve a more uniform current distribution and limit AC losses.

The analyses have shown that the natural transposition that occurs in these specific conductors, either on one side of the bundle or on both, significantly reduces losses. However, above a certain frequency, it becomes necessary to use a more advanced approach by adopting wire windings or even Litz wire windings. The thesis also considered the use of bars made of Litz wires to conduct comparative analyses with Hairpin windings. Furthermore, low number of turns concentrated-coil windings machine were considered and conductor subdivision was explored to determine the optimal arrangement for reducing AC losses.
Finally, a reduced static test-rig to validate the calculation tool was designed, although lead times in the supply chain have not allow to build it on time before the conclusion of the project.
Despite the promising results, more research is yet needed on the subject. Conducting some experimental validation with the proposed test-rig is certainly a priority. Additionally the calculation tool may be expanded to incorporate the effects of the PM rotating field on losses, which would allow a more robust optimisation especially in motor designs with high saturation factors. Another important direction for future development concerns the analysis of the thermal behaviour of the windings, especially those made of Litz wire.

References

[1] T. Guillod, J. Huber, F. Krismer and J. W. Kolar, "Litz wire losses: Effects of twisting imperfections", *Proc. IEEE 18th Workshop Control Model. Power Electron.*, pp. 1-8, 2017.

[2] J. Gyselinck and P. Dular, "Frequency-domain homogenization of bundles of wires in 2-D magnetodynamic FE calculations", *IEEE Trans. Magn*, vol. 41, no. 5, pp. 1416-1419, May 2005.

[3] D Meeker, "Continuum Representation of Wound Coils via an Equivalent Foil Approach"

[4] Advanced propulsion centre UK, "Electric Machines Roadmap"

[5] N. Bianchi, G. Berardi, "Analytical Approach to Design Hairpin Windings in High Performance Electric Vehicle Motors"